Supplementary Material:

Conformational selection governs the binding preferences of imatinib for several tyrosine kinases

Alexey Aleksandrov and Thomas Simonson
Laboratoire de Biochimie (CNRS UMR7654), Department of Biology, Ecole Polytechnique, 91128 Palaiseau, France.

Section 1, below, reports PBFE calculations of Abl binding by several imatinib analogues; these calculations provide an additional test of the PBFE method for imatinib:kinase binding. **Section 2** reports PBFE calculations that compare imatinib binding to Abl in its DFG-out and DFG-in inactive conformations. This analysis will allow us to prove, in the case of Abl, one of the assumptions we introduced in the main text, assumption **(B1)**: $\Delta G_1^{\rm conf}(\text{Abl}) \geq 1$ kcal/mol. The DFG-out complex and its interactions with imatinib are described first. We then propose a model for the complex of imatinib with DFG-in Abl, for which there is no experimental structure. Finally, we estimate the DFG-in/DFG-out binding free energy difference, and discuss its relation to the conformational free energies $\Delta G_0^{\rm conf}(\text{Abl})$ and $\Delta G_1^{\rm conf}(\text{Abl})$. This discussion allows us to prove **(B1)**.

1. Imatinib analogues binding to Abl: additional PBFE testing

As an additional test of the simple, PBFE method, we report calculations for four imatinib analogues binding to Abl [1]. The imatinib variations involve three positions, circled in Figure 1; we refer to them as R2H, X1N, R1Cl, and R1M. In R2H, the C17 methyl is replaced by a hydrogen. In X1N, the C9H group in ring E is replaced by a nitrogen atom. In R1Cl, chloride replaces the hydrogen in the C28H group. In R1M, there is a new methyl on C28. Earlier, we described the force field parameterization of the analogues, as well as rigorous, MDFE calculations of their relative binding free energies [1]. Here, we compare PBFE to the MDFE data and to experimental data when available. Results are given in Table 1. PBFE uses both a continuum dielectric and a nonpolar free energy term. The nonpolar term is a surface area term (see main text); the best agreement is obtained with an atomic surface coefficient of 50 cal/mol/Å^2. PB uses a protein dielectric of four; slightly worse agreement is obtained with a value of six (not shown). PBFE conformations were taken from earlier MD simulations [1]. The rms deviation between PBFE and MDFE is 1.0 kcal/mol. The agreement between

PBFE and experiment (when available) is similar. In the main text, we assume a slightly larger uncertainty of ±1.5 kcal/mol for the PBFE free energies, based on these and earlier accuracy tests [2–5].

Table 1: Imatinib analogues binding to Abl: MDFE, PBFE, and experiment

imatinib	MDFE			experiment	PBFE
modification	$^a\Delta G_{prot}$	$^a\Delta G_{sol}$	$\Delta\Delta G$	$\Delta\Delta G_{exp}$	$^c\Delta\Delta G$
X1N	-5.4	-5.4	0.0	-0.1^b [6]	0.2 (0.2/0.0)^c
R1Cl	4.6	7.4	-2.8	-2.8,-1.8^b [6, 7]	-1.9 (-0.3/-1.6)
R2H	-4.2	-5.8	1.6	-	1.5 (0.3/1.2)
R1M	0.5	3.2	-2.7	-	-1.0 (-0.3/-0.7)

Free energies in kcal/mol. ^{a}Columns 3, 4 are the free energy to reversibly transform plain imatinib into one of its analogues, either in the protein (ΔG_{prot}) or in solution (ΔG_{sol}). $\Delta\Delta G = \Delta G_{prot} - \Delta G_{sol}$ is the relative binding free energy. A negative $\Delta\Delta G$ means the analogue binds more strongly than imatinib. MDFE error bars are all close to 0.3 kcal/mol. ^{b}Derived from Minimum Inhibitory Concentration *in vivo*. ^{c}In parentheses, the electrostatic/nonpolar contributions are given separately. The protein dielectric is ϵ_P=4; the atomic surface free energy is 50 cal/mol/Å^2.

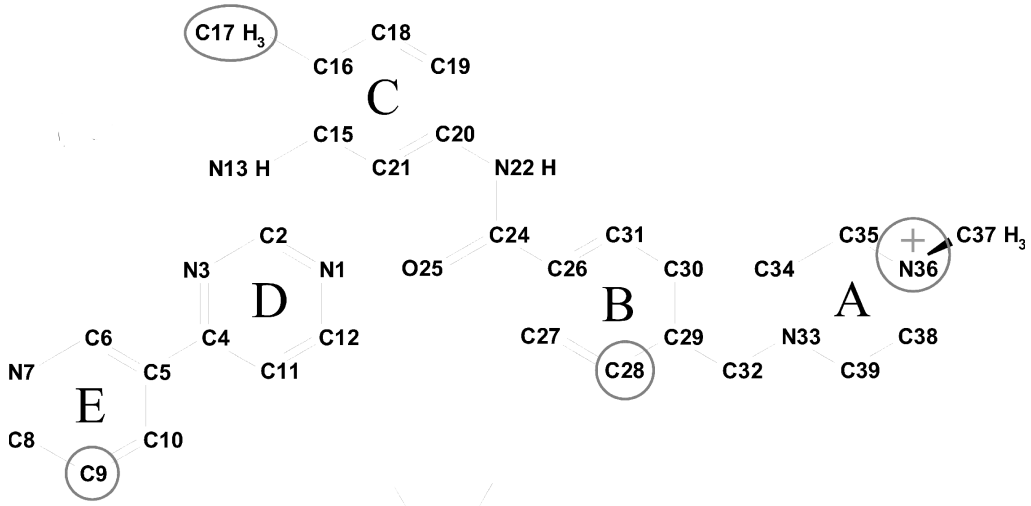

Figure 1: 2D view of imatinib. Positions modified in this work are circled. Also circled is N36, which is protonated and positively-charged.

2. Imatinib binds weakly to Abl in the DFG-in inactive conformation; proof of assumption B1

In this section, we compare imatinib binding to the DFG-in and DFG-out inactive conformations of Abl. The corresponding binding free energy difference will be denoted $\Delta\Delta G^{\rm conf}$. Using the thermodynamic cycle and the notations of Fig. 2 in the main text, we have

$$\Delta\Delta G^{\rm conf} = \Delta G^{\rm In}_{\rm bind} - \Delta G^{\rm Out}_{\rm bind} = \Delta G^{\rm conf}_1 - \Delta G^{\rm conf}_0. \quad (1)$$

Our main goal is not to obtain a very precise estimate of $\Delta\Delta G^{\rm conf}$, but rather to show that it is large, 5 kcal/mol at least (see below). This will allow us to prove assumption **(B1)** in the case of Abl. In addition to this main goal, we will use this section to describe in more detail some of the protein-ligand interactions that are present in the DFG-out complex, and to describe our model of the protein-ligand complex when Abl is in its DFG-in state. Finally, we will consider the relation to assumption **(B1)**.

Imatinib binding to DFG-out Abl: PBFE binding free energy We first consider imatinib binding to Abl in its DFG-out inactive conformation, using the PBFE approach. The protein is subjected to molecular dynamics simulation, surrounded by a bath of explicit water molecules. The resulting conformations are used as input for a Poisson-Boltzmann free energy estimation, where the protein and solvent are described as two distinct dielectric media [2, 8, 9]. The MD simulation was run for 5 ns. The structure remains very similar to the initial, X-ray structure, with an rms deviation of just 1.0 Å for backbone atoms within 10 Å of the imatinib ligand. Imatinib itself shifts by just 0.5 Å. The interactions characteristic of the DFG-out conformation are maintained: the Lys271–Glu286 salt bridge; a hydrogen bond between Glu286 and N22 in the positively-charged piperazine A ring of imatinib (Figure 2); two hydrogen bonds between the protein backbone and imatinib: N(M318)–N3(Ima) and O_γ(T315)–N8(Ima). The piperazine ring is further stabilized by interactions with the backbones of Ile360 and His361, and by long-range electrostatic interactions with Asp381 in the DFG motif.

The electrostatic component of the Abl binding free energy is estimated to be -15.3 kcal/mol. This free energy can be decomposed further into a sum of terms, associated with different Abl amino acids [10, 11]. The largest components come from Glu286 and Asp381: respectively 34% (-5.3 kcal/mol) and 19% (-2.9 kcal/mol) of the total. Glu286 interacts with imatinib through the N21, C17, and C29 hydrogens. Asp381 has favorable long-range electrostatic interactions with protonated imatinib. The back-

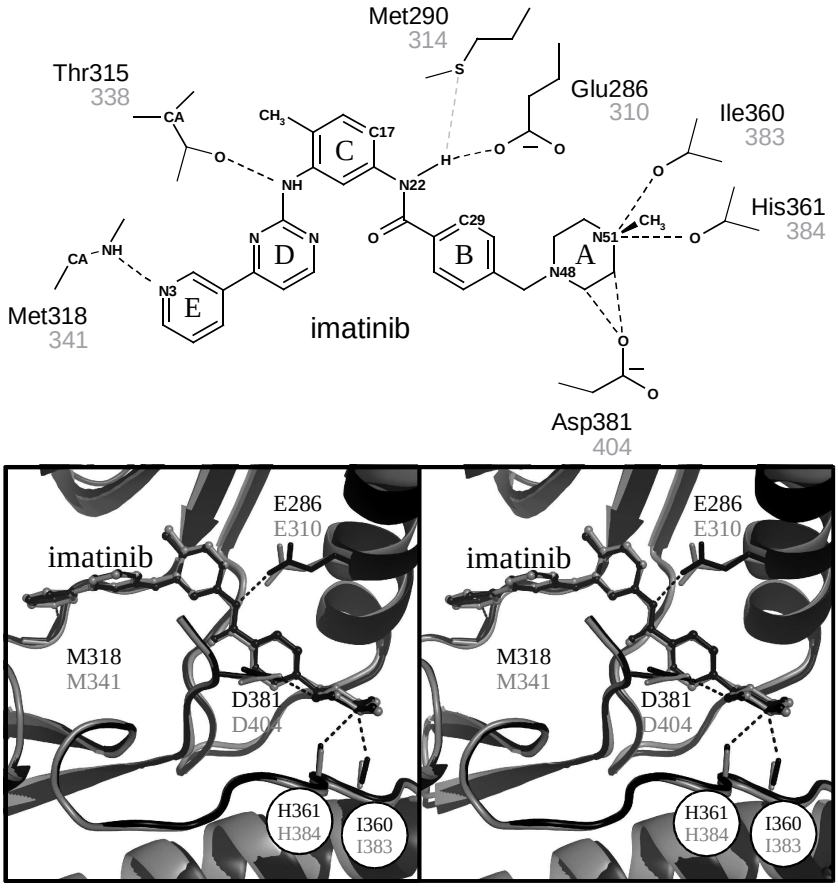

Figure 2: Binding site residues in DFG-out Abl (black) and Src (gray); 2D and 3D (stereo) views. Both human Abl (black) and chicken Src (gray) numbering are given.

bone groups of Ile360 and His361, which anchor the charged imatinib piperazine ring, together contribute 26% of the total energy (-4.0 kcal/mol). Thr315 (which confers imatinib resistance when mutated to isoleucine [12]) contributes just 6% (-1.0 kcal/mol) of the total free energy. Imatinib also interacts with the backbones of Met318 and Ala380, which contribute -1.4 kcal/mol and -1.2 kcal/mol, respectively. Met290, whose interaction with imatinib is shown in Fig. 2, contributes just 0.2 kcal/mol to binding.

Imatinib binding to DFG-in Abl: structural model Imatinib binding to Abl in the DFG-in inactive conformation is thought to be weak or non-existent, and there is no experimental structure of such a complex. To model this state, imatinib was added to the Abl structure in its DFG-in inactive conformation, based on a least-squares

superposition with the Abl:imatinib X-ray complex. During the superposition, Cα atoms within 10 Å of imatinib were considered. The resulting structure was energy-minimized with harmonic restraints applied to the entire protein but not to imatinib. An MD simulation was then performed for 5 nanoseconds. After 5 ns, the structure was compared to the initial model. The root mean square deviation for backbone atoms within 10 Å of imatinib was just 0.9 Å. The rms deviation for imatinib was 0.9 Å, arising mainly from a rotation of the piperazine A ring. Excluding this ring, the rms deviation was just 0.6 Å, comparable to the DFG-out inactive case, above. Thus, only small deformations are needed to build an imatinib complex with Abl in its DFG-in, Src-like inactive conformation. The stability of the simulation on the nanosecond timescale confirms that the DFG-in structure is a local minimum on the protein's conformational free energy surface. If the simulation were much longer, the protein would escape from this minimum and convert into the DFG-out conformation [13].

The resulting DFG-in model of Abl with bound imatinib is illustrated in Fig. 3. Several interactions are modified, compared to the DFG-out conformation, accounting for the weaker binding. During the first 10 ps of dynamics, the salt bridge between Lys271 and Asp381 breaks. This salt bridge is characteristic of the Src-like inactive state, where it narrows the imatinib binding pocket. The hydrogen bond between Glu286 and the imatinib piperazine A ring, found in the DFG-out conformation, is not formed here. Rather, Glu286 points out of the imatinib pocket and forms a salt bridge with Arg386, characteristic of the DFG-in conformation (Glu310–Arg409 in human c-Src) [14]; this salt bridge is maintained throughout the MD simulation. Two other protein–ligand hydrogen bonds found in the DFG-out conformation are preserved here: N(M318)–N3(Ima) and O_γ(T315)–N8(Ima), with mean distances of 3.1 and 3.0 Å, respectively; the same as in the DFG-out conformation, above.

The Glu286–Arg386 salt bridge shifts the DFG loop towards Glu286; this, in turn, prohibits the interaction between the imatinib piperazine ring and Ile360 and His361. The N22 atom of imatinib, instead of interacting with Glu286 as in the DFG-out conformation, finds itself in a hydrophobic pocket formed by the sidechains of Met290, Ile313, Leu384, and Leu387. The central DFG residue, Phe382, which overlaps with the imatinib binding site in the DFG-in conformation of apo-Src and apo-Abl, has rotated to position itself in a hydrophobic pocket formed by Ile293, Leu298, Val299 and Leu354. The shortest distance between imatinib and Phe382 is 3.4 Å. Fig. 3 illustrates the absence of steric clashes between imatinib and the repositioned Phe382. The ability of Phe382 to reorient at a moderate energy cost contradicts the notion

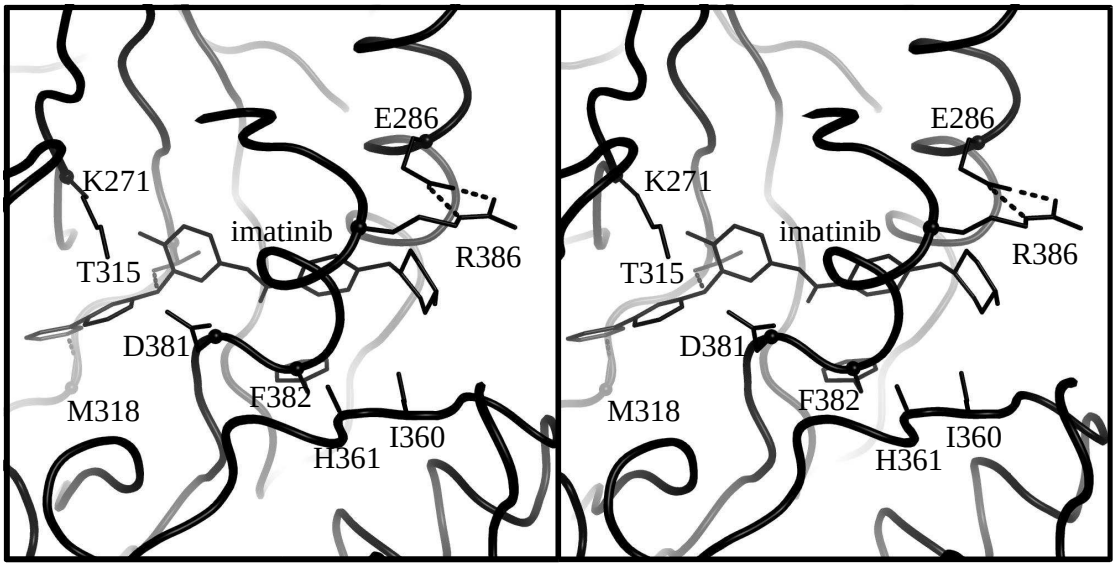

Figure 3: Imatinib bound to the DFG-in inactive conformation of Abl; a representative snapshot from a molecular dynamics simulation (stereo view).

that Phe382 completely blocks imatinib binding to the DFG-in conformation. Indeed, it was found experimentally that the mutation of this residue to alanine improves the imatinib:Src binding affinity by just 1.0 kcal/mol [15].

Imatinib binding to DFG-in Abl: contribution of the Lys271–Asp381 salt bridge Below, we use PBFE to compute the imatinib binding free energy to Abl in its DFG-in inactive state (more precisely, the electrostatic contribution to binding). In the DFG-in state, a new salt bridge forms once the ligand is removed, Lys271–Asp381. Its contribution would be largely neglected by the usual PBFE method. Thus, for the imatinib unbinding reaction in the DFG-in state, we use a 3-step protocol. First, we reversibly introduce a restraint potential to control the Lys271–Asp381 distance and prevent salt bridge formation. This is done over a series of MD simulations (with explicit solvent). Second, we remove the ligand, treating this step with PBFE. Because of the restraint, the protein structure does not change when the ligand is removed; thus, the usual PBFE protocol should be appropriate. Third, we slowly remove the restraint, during the course of another MD simulation. The free energies for steps one and three are computed from standard free energy perturbation theory [16].

More specifically, the restraint potential is a one-sided, harmonic restraint, which

penalizes distances between Lys271-NZ and the Asp381-OD1 and -OD2 shorter than a target distance d, with a force constant of 6 kcal/mol/Å^2. The restraint is imposed initially by increasing the force constant over a series of MD simulations totalling 3 ns (with the same, explicit solvent protocol used throughout this paper). The target distance d is then gradually reduced from 4.5 to 2.5 Å over another series of MD simulations, totalling 6 nanoseconds. Once the target distance reaches 2.5 Å, the restraint energy is always zero (within the precision of the calculation) so that the restraint has effectively been removed [16].

Imatinib binding to DFG-in Abl: PBFE binding free energy and comparison to DFG-out The PBFE calculations then yield a binding free energy contribution of -11.0±0.8 kcal/mol, not including the contribution of the Lys271–Asp381 salt bridge in the apo state. The latter contribution is found to be +3.9±0.6 kcal/mol, opposing binding. For DFG-out binding, above, we obtained a PBFE estimate of -15.3 kcal/mol. Overall, the difference between DFG-in and DFG-out binding is $\Delta\Delta G^{\rm conf}$ = +8.2 kcal/mol. Since protein relaxation is also included in the PBFE model, the MDFE estimate of the Lys271–Asp381 salt bridge contribution should probably be viewed as an upper limit. Indeed, experimental estimates of salt bridge contributions to protein stability are usually smaller, closer to 1 kcal/mol [17]. Therefore, we conclude that $\Delta\Delta G^{\rm conf}$ is somewhere between 5 and 8 kcal/mol. The nonpolar contribution to $\Delta\Delta G^{\rm conf}$ is 0.4 kcal/mol, using the surface area model with a large atomic surface free energy of 50 cal/mol/Å^2. If we use a different model for the nonpolar term, the Linear Interaction Energy Model (see main text), we obtain a similar, small nonpolar contribution of 0.1 kcal/mol.

Imatinib binding to DFG-in and DFG-out Abl: relation to $\Delta G_1^{\rm conf}$(Abl) and assumption B1 We saw above that $\Delta\Delta G^{\rm conf} = \Delta G_1^{\rm conf}$ - $\Delta G_0^{\rm conf}$, so that

$$\Delta G_1^{\rm conf} = \Delta G_0^{\rm conf} + \Delta\Delta G^{\rm conf}. \quad (2)$$

Experimentally, we know that $\Delta G_0^{\rm conf} > 0$, since apo-Abl prefers to be DFG-out. Since $\Delta\Delta G^{\rm conf} \geq 5$ kcal/mol, we see that $\Delta G_1^{\rm conf}$ is also greater than 5 kcal/mol. Even allowing for a sizeable PBFE uncertainty, we may confidently conclude that **(B1)** is verified for Abl: $\Delta G_1^{\rm conf} \geq 1$ kcal/mol.

References

[1] Aleksandrov, A., and Simonson, T. A molecular mechanics model for imatinib and imatinib:kinase binding. *J. Comp. Chem. in press* (2010), 0000.

[2] Simonson, T., Archontis, G., and Karplus, M. Free energy simulations come of age: the protein–ligand recognition problem. *Acc. Chem. Res. 35* (2002), 430–437.

[3] Hunenberger, P., Helms, V., Narayana, N., Taylor, S., and McCammon, J. Determinants of ligand binding to cAMP-dependent protein kinase. *Biochemistry 38* (1999), 2358–2366.

[4] Wong, C., Hunenberger, P., Akamine, P., Narayana, N., Diller, T., McCammon, J., Taylor, S., and Xuong, N. Computational analysis of PKA–balanol interactions. *J. Med. Chem. 44* (2001), 1530–1539.

[5] Pearlman, D. A. Evaluating the Molecular Mechanics Poisson-Boltzmann Surface Area free energy method using a congeneric series of ligands to p38 MAP kinase. *J. Med. Chem. 48* (2005), 7796–7807.

[6] Asaki, T., Sugiyama, Y., Hamamoto, T., Higashioka, M., Umehara, M., Naito, H., and Niwa, T. Design and synthesis of 3-substituted benzamide derivatives as Bcr-Abl kinase inhibitors. *Bioorg. Med. Chem. Lett. 16* (2006), 1421–1425.

[7] Puttini, M., Redaelli, S., Moretti, L., Brussolo, S., Gunby, R., Mologni, L., Marchesi, E., Cleris, L., Donella-Deana, A., Drueckes, P., Sala, E., Lucchini, V., Kubbutat, M., Formelli, F., Zambon, A., Scapozza, L., and Gambacorti-Passerini, C. Characterization of compound 584, an Abl kinase inhibitor with lasting effects. *Haematologica 93* (2008), 653–661.

[8] Simonson, T. Free energy calculations: approximate methods for biological macromolecules. In *Free energy calculations: theory and applications in chemistry and biology*, C. Chipot and A. Pohorille, Eds. Springer Verlag, N.Y., 2007, ch. 12.

[9] McCammon, J. Computation of noncovalent binding affinities. In *Theory and Applications of Computational Chemistry*, C. Dykstra, G. Frenking, K. Kim, and G. Scuseria, Eds. Elsevier, Amsterdam, 2005, pp. 41–46.

[10] Hendsch, Z., and Tidor, B. Electrostatic interactions in the GCN4 leucine zipper: substantial contributions arise from intramolecular interactions enhanced on binding. *Prot. Sci. 8* (1999), 1381–1392.

[11] Archontis, G., Simonson, T., and Karplus, M. Binding free energies and free energy components from molecular dynamics and Poisson-Boltzmann calculations. Application to amino acid recognition by aspartyl-tRNA synthetase. *J. Mol. Biol. 306* (2001), 307–327.

[12] Gorre, M. E., Mohammed, M., Ellwood, K., Hsu, N., Paquette, R., Rao, P. N., and Sawyers, C. L. Clinical resistance to STI-571 cancer therapy caused by BCR-ABL gene mutation or amplification. *Science 293* (2001), 876–880.

[13] Shan, Y., Seeliger, M. A., Eastwood, M. P., Frank, F., Xu, H., Jensen, M. O., Dron, R. O., Kuriyan, J., and Shaw, D. E. A conserved protonation-dependent switch controls drug binding in the Abl kinase. *Proc. Natl. Acad. Sci. USA 106* (2009), 139–144.

[14] Xu, W., Doshi, A., Lei, M., Eck, M. J., and Harrison, S. C. Crystal structures of c-Src reveal features of its auto-inhibitory mechanism. *Molec. Cell 3* (1999), 629–638.

[15] Seeliger, M. A., Nagar, B., Frank, F., Cao, X., Henderson, M. N., and Kuriyan, J. c-Src binds to the cancer drug imatinib with an inactive Abl/c-Kit conformation and a distributed thermodynamic penalty. *Structure 15* (2007), 299–311.

[16] Simonson, T. Free energy calculations. In *Computational Biochemistry & Biophysics*, O. Becker, A. Mackerell Jr., B. Roux, and M. Watanabe, Eds. Marcel Dekker, N.Y., 2001, ch. 9.

[17] Fersht, A. *Structure and mechanism in protein science: a guide to enzyme catalysis and protein folding.* Freeman, New York, 1999.